

End-to-End Environmental Sound Classification using a 1D Convolutional Neural Network

Sajjad Abdoli¹, Patrick Cardinal, Alessandro Lameiras Koerich

Department of Software and IT Engineering, École de Technologie Supérieure, Université du Québec, H3C 1K, Montreal, QC, Canada

Abstract

In this paper, we present an end-to-end approach for environmental sound classification based on a 1D Convolution Neural Network (CNN) that learns a representation directly from the audio signal. Several convolutional layers are used to capture the signal's fine time structure and learn diverse filters that are relevant to the classification task. The proposed approach can deal with audio signals of any length as it splits the signal into overlapped frames using a sliding window. Different architectures considering several input sizes are evaluated, including the initialization of the first convolutional layer with a Gammatone filterbank that models the human auditory filter response in the cochlea. The performance of the proposed end-to-end approach in classifying environmental sounds was assessed on the UrbanSound8k dataset and the experimental results have shown that it achieves 89% of mean accuracy. Therefore, the proposed approach outperforms most of the state-of-the-art approaches that use handcrafted features or 2D representations as input. Moreover, the proposed approach outperforms all approaches that use raw audio signal as input to the classifier. Furthermore, the proposed approach has a small number of parameters compared to other architectures found in the literature, which reduces the amount of data required for training.

Keywords: Convolutional neural network, Environmental sound classification, Deep learning, Gammatone filterbank.

Abbreviations: AI: Air conditioner; BC: Between Class; CA: Car horn; CH: Children playing; CST: Chroma, Spectral contrast, Tonnetz; CNN: Convolution Neural Network; CRP: Cross Recurrence Plot; DS: Dempster-Shafer; DO: Dog bark; DR: Drilling; EN: Engine; GU: Gun shot; JA: Jackhammer; LMC: LM, CST; LM: Log-Mel; MFCC: Mel-Frequency Cepstral Coefficients; MC: MFCC, CST; SI: Siren; SKM: Spherical K-Means; ST: Street music; SVMs: Support Vector Machines.

Email addresses: sajjad.abdoli.1@ens.etsmtl.ca (Sajjad Abdoli), patrick.cardinal@etsmtl.ca (Patrick Cardinal), alessandro.koerich@etsmtl.ca (Alessandro Lameiras Koerich)

¹Corresponding author

1. Introduction

In the last years, Convolutional Neural Networks (CNNs) have had significant impact on several audio and music processing tasks such as automatic music tagging (Dieleman & Schrauwen, 2014), large-scale video clip classification based on audio information (Hershey et al., 2017), music genre classification (Costa et al., 2017), speaker identification (Ravanelli & Bengio, 2018), environmental sound classification (Piczak, 2015a; Salamon & Bello, 2017; Pons & Serra, 2018; Simonyan & Zisserman, 2014; Tokozume et al., 2017; Esmaeilpour et al., 2019b), among others. Environmental sound classification is an interesting problem (Sigtia et al., 2016; Stowell et al., 2015) which has different applications ranging from crime detection (Radhakrishnan et al., 2005) to environmental context aware processing (Chu et al., 2009). Moreover, with the increasing interest in smart cities, IOT devices embedding automatic audio classification can be very useful for urban acoustic monitoring (Mydlarz et al., 2017) like intelligent audio-based surveillance system in public transportation (Laffitte et al., 2019).

Like typical automatic classification systems, most of the approaches for environmental sound classification rely on handcrafted features or learn representations from mid-level representations such as spectro-temporal features (Ludeña-Choez & Gallardo-Antolín, 2016; Costa et al., 2012). Spectral representations have been used as features in several approaches based on matrix factorization (Mesaros et al., 2015; Benetos et al., 2016; Bisot et al., 2016; Salamon & Bello, 2015; Geiger & Helwani, 2015). Mesaros et al. (2015) presented an approach for overlapping sound event detection based on learning non-negative dictionaries through joint use of spectrum and class activity annotation. Benetos et al. (2016) presented an approach for overlapping acoustic event detection based on probabilistic latent component analysis where each exemplar in a sound event dictionary consists of a succession of spectral templates. Bisot et al. (2016) learn features from time-frequency images in an unsupervised manner. The images are decomposed using matrix factorization methods to build a dictionary and the projection coefficients are used as features for classification. Salamon & Bello (2015) proposed a dictionary learning method based on the Spherical K-Means (SKM) algorithm which used log-Mel spectrograms as input. Geiger & Helwani (2015) used Gabor filterbank features and Gaussian Mixture Models for event detection. Mulimani & Koolagudi (2019) used a singular value decomposition method for extracting acoustic event specific features from spectrogram. These features are used as input to a Support Vector Machine (SVM) classifier. Recently, Xie & Zhu (2019) proposed a method for aggregation of acoustic and visual features for acoustic scene classification. Several acoustic features like spectral centroid, spectral entropy as well as several visual features like local binary pattern, histogram of gradients are proposed. A suitable feature selection algorithm like principle component analysis is also used. The selected feature set is used as input to an SVM classifier.

Recent works explore CNN-based approaches given the significant improvements over hand-crafted feature-based methods (Piczak, 2015a; Salamon & Bello, 2017; Pons & Serra, 2018; Simonyan & Zisserman, 2014; Tokozume et al., 2017). However, most of

43 these approaches first convert the audio signal into a 2D representation (spectrogram)
44 and use 2D CNN architectures that were originally designed for object recognition such
45 as AlexNet and VGG (Simonyan & Zisserman, 2014; Boddapati et al., 2017). One of the
46 main advantages of using 2D representations is that spectrograms can summarize high
47 dimensional waveforms into a compact representation (Costa et al., 2011). Furthermore,
48 1D representations are noisier compared to 2D representations (Stowell & Plumbley,
49 2014). Piczak (Piczak, 2015a) presented a CNN with two layers followed by three dense
50 layers. The network operates on two input channels: log-Mel spectra and their deltas.
51 However, one of the challenges in using 2D CNNs for environmental sound classification
52 is that the modelling capacity of such networks depends on the availability of a large
53 amount of training data to learn kernel parameters without over-fitting. The scarcity
54 of labeled data of environmental sounds is also a problem. Salamon & Bello (2017)
55 presented a method based on a 2D CNN with five layers (SB-CNN) where new training
56 samples are generated using data augmentation methods such as time stretching, pitch
57 shifting, dynamic range compression or adding background noise (McFee et al., 2015).
58 The 2D CNN was trained on the augmented dataset and evaluated on the original
59 samples. They reported the classification accuracy of 79% on a dataset of environmental
60 sounds (Salamon et al., 2014). Pons & Serra (2018) used randomly weighted 2D CNNs
61 (non-trained) for extracting features from audio spectrograms and raw audio samples
62 for sound classification. Several experiments have been conducted to find the best
63 architectures for this method. In the case of environmental sound classification, the best
64 results have been obtained by using a VGG 2D CNN (Simonyan & Zisserman, 2014)
65 as a feature extractor and SVMs as classifiers. They reported mean accuracy of 70%
66 for this problem. Boddapati et al. (2017) used spectrogram, Mel-Frequency Cepstral
67 Coefficients (MFCC) and Cross Recurrence Plot (CRP) and AlexNet and GoogLeNet for
68 classification of 2D representations of environmental sounds. They reported accuracy
69 between 92% and 93% on classifying environmental sounds. Tokozume et al. (2017)
70 proposed a new method called Between-Class (BC) learning for training neural networks.
71 The network, for which the input is a mixture of two audio samples, is trained to predict
72 the mixing ratio of the samples. According to their experiments, the BC learning has
73 shown performance improvement for various architectures used for sound identification
74 tasks. They also proposed an end-to-end 1D CNN (EnvNet-v2) that performs well on
75 various environmental sound datasets when trained with the BC learning approach,
76 compared to conventional learning techniques. The best error rate of 8.6% is reported
77 on ESC-10 dataset (Piczak, 2015b).

78 1D CNNs that learn acoustic models directly from audio waveforms are becoming
79 a popular method in audio processing due to the ability of these networks to take
80 advantage of the signal’s fine time structure (Hoshen et al., 2015). Kim et al. (2018)
81 proposed a 1D CNN architecture for music auto-tagging inspired by the building blocks
82 of Resnets (He et al., 2016) and SENets (Hu et al., 2018). Zhu et al. (2016) proposed an
83 end-to-end learning approach for speech recognition based on multiscale convolutions
84 that learns the representation directly from audio waveforms. Three 1D convolutional

85 layers with different kernel sizes are used for feature extraction and the features are
86 concatenated by a pooling layer for ensuring a consistent sampling frequency for the
87 rest of the network. They reported 23.28% of word error rate on a dataset drawn
88 from a collection of sources including read, conversational, accented, and noisy speech.
89 Ravanelli and Bengio (Ravanelli & Bengio, 2018) proposed the SincNet, an end-to-end
90 approach for speaker identification and verification. The first layer of such a model is
91 based on parametric sinc functions, which are band-pass filters. Only low and high cutoff
92 frequencies of the filters are learned from data. This model learns meaningful filters for
93 the first layer and decreases the number of parameters of the model. This model achieves
94 a sentence error rate of 0.85% on TIMIT dataset (Garofolo et al., 1993). Zeghidour
95 et al. (2018) also proposed an end-to-end 1D CNN architecture for speech recognition
96 by learning a filter bank which is considered as a replacement of Mel-filterbanks. Hoshen
97 et al. (2015) proposed an end-to-end multichannel 1D CNN for speech recognition. They
98 also found that the timing difference between channels is an indicator of the location of
99 the input in space. They reported 27.1% of single channel word error rate on a large
100 vocabulary voice search dataset. Sainath et al. (2015) used a similar architecture for
101 speech recognition. They showed that features learned directly from the audio waveform
102 match the performance of log-Mel filterbank energies. Dai et al. (2017) proposed several
103 very deep convolutional models for environmental sound classification that achieved
104 72% of accuracy on UrbanSound8k dataset. The proposed models consist of batch
105 normalization, residual learning, and down-sampling in the initial layers of the CNN.

106 The prediction of two CNNs that learn from raw audio and 2D representations
107 of the signal can also be combined to achieve a robust prediction. Li et al. (2018)
108 combined one network that learns directly from audio waveform (RawNet) and one
109 network that learns high level representations from log-Mel features (MelNet). The
110 models are trained independently and the prediction of the two models is combined
111 using the Dempster–Shafer (DS) method. This ensemble method produces 92.2%, 92.6%
112 and 83.1% of accuracy on UrbanSound8k (Salamon et al., 2014), ESC-10 and ESC-50
113 (Piczak, 2015b) datasets, respectively. Su et al. (2019) proposed the TSCNN-DS model,
114 which also combined the prediction of two CNNs using the DS method. Five auditory
115 features such as Log-Mel spectrogram (LM), MFCC, Chroma, Spectral contrast and
116 Tonnetz (CST) are extracted from the audio signal. LM and CST are stacked and
117 considered as one feature set (LMC). Likewise, MFCC and CST (MC) features are also
118 combined by stacking. The two feature sets are used for training two identical four-
119 layer CNNs. The prediction of the CNNs are then combined using the DS method. The
120 TSCNN-DS achieves the classification accuracy of 97.2% on UrbanSound8k dataset.

121 In this paper, we propose an end-to-end 1D CNN for environmental sound classifi-
122 cation that learns the representation directly from the audio signal instead of from 2D
123 representations (Piczak, 2015a; Salamon & Bello, 2017, 2015). The proposed end-to-end
124 approach provides a compact architecture that reduces the computation cost and the
125 amount of data required for training. With the aim of extracting relevant information
126 directly from audio waveforms, several convolutional layers are used to learn low-level

127 and high-level representations. The highest level of representation is then used for clas-
128 sifying the input signal by means of three fully connected layers. Experimental results
129 on UrbanSound8k dataset, which contains 8,732 environmental sounds from 10 classes,
130 have shown that the proposed approach outperforms other approaches based on 2D
131 representations such as spectrograms (Piczak, 2015a; Salamon & Bello, 2017; Pons &
132 Serra, 2018; Salamon & Bello, 2015) by between 11.24% (SB-CNN) and 27.14% (VGG)
133 in terms of mean accuracy. Furthermore, the proposed approach does not require data
134 augmentation or any signal pre-processing for extracting features.

135 Our contribution in this paper is twofold. We present an end-to-end 1D CNN initial-
136 ized with Gammatone filterbanks that has few parameters and which does not require
137 a large amount of data for training compared to dense 2D CNNs which have millions of
138 trainable parameters. Besides, it achieves state-of-the-art performance. Secondly, the
139 proposed approach can handle audio signals of any length by using a sliding window
140 of appropriate width that breaks up the audio signal into short frames of dimension
141 compatible with the input layer of the end-to-end 1D CNN.

142 This paper is organized as follows. Section 2 presents the ideas behind the proposed
143 end-to-end 1D CNN architecture and the proposed approach to deal with variable audio
144 lengths. We also present the variations in the architecture that may arise from different
145 input dimensions as well the process of aggregating the predictions on audio frames.
146 Section 3 presents the benchmarking dataset, the experimental protocol, the procedure
147 used to fine-tune the proposed 1D CNN to the data, the evaluation of different input
148 sizes, the enhancements in the proposed 1D CNN to improve its performance and an
149 analysis of the frequency response of the filters learned at the different convolutional
150 layers. In Section 4, we compare the performance of the proposed approach with the
151 state-of-the-art in environmental sound classification and we analyze the magnitude
152 responses of the filters learned at the first convolutional layer to gain some insight on
153 the behaviour of the proposed 1D CNN. Finally, the conclusions and perspectives of
154 future work are presented in the last section.

155 2. Proposed End-to-End Architecture

156 The aim of the proposed end-to-end architecture is to handle audio signals of variable
157 lengths, learning directly from the audio signal, a discriminative representation that
158 achieves a good classification performance on different environmental sounds.

159 2.1. Variable Audio Length

160 One of the challenges of using 1D CNNs in audio processing is that the length of
161 the input sample must be fixed but the sound captured from the environment may have
162 various duration. Therefore, it is necessary to adapt a CNN to be used with audio
163 signals of different lengths. Moreover, a CNN must be used for continuous prediction of
164 input audio signals of environmental sounds.

165 One way to circumvent this constraint imposed by the CNN input layer is to split
166 the audio signal into several frames of fixed length using a sliding window of appropriate

167 width. Therefore, in our approach we use a window of variable width to conditionate
 168 the audio signal to the input layer of the proposed 1D CNN. The window width depends
 169 mainly on the signal sampling rate. Furthermore, successive audio frames may also have
 170 a certain percentage of overlapping, which aim is to maximize the use of information.
 171 This naturally increases the number of samples as some parts of the audio signal are
 172 reused and that can be viewed as some sort of data augmentation. The process of
 173 framing the audio signal into appropriate frames is illustrated in Figure 1.

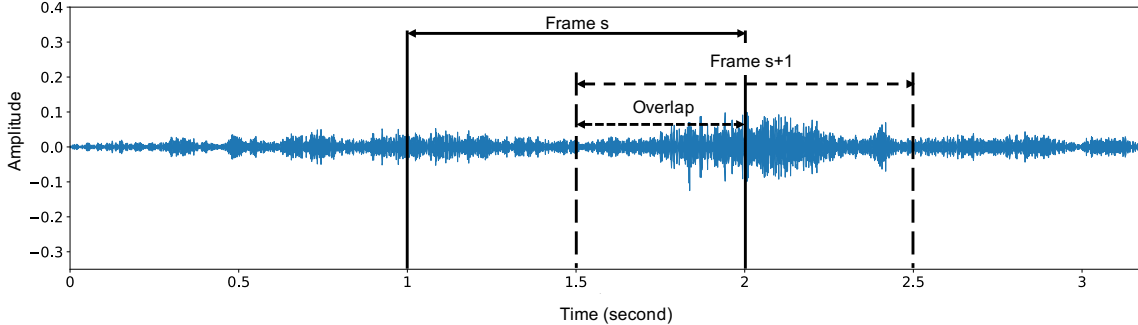


Figure 1: Framing the input audio signal into several frames ($s, s + 1$) with appropriate overlapping percentage (50%).

174 Moreover, the sampling rate of the audio signals has a direct impact on the dimen-
 175 sionality of the input sample and eventually on the computational cost of model. For
 176 environmental sounds, a sampling rate of 16 kHz may be considered a good trade-off
 177 between the quality of the input sample and the computational cost of the model.

178 2.2. 1D CNN Topology

179 A 1D CNN is analogous to a regular neural network but but it has generally raw data
 180 as input instead of handcrafted features. Such an input data is processed through several
 181 trainable convolutional layers for learning an appropriate representation of the input.
 182 According to the "local connectivity" theorem, the neurons in a layer are connected only
 183 to a small region of the previous layer. This small region of connectivity is called a
 184 receptive field. The input to out 1D CNN is an array representing the audio waveform,
 185 which is denoted as X . The network is designed to learn a set of parameters Θ to map
 186 the input to the prediction T according to a hierarchical feature extraction given by
 187 Equation 1:

$$T = F(X | \Theta) = f_L(\dots f_2(f_1(X | \Theta_1) | \Theta_2) | \Theta_L) \quad (1)$$

188 where L is the number of hidden layers in the network. For the convolutional layers,
 189 the operation of the l -th layer can be expressed as:

$$T_l = f_l(X_l | \Theta_l) = h(W \otimes X_l + b), \quad \Theta_l = [W, b] \quad (2)$$

190 where \otimes denotes the convolution operation, X_l is a two-dimensional input matrix of
 191 N feature maps, W is a set of N one dimensional kernels (receptive field) used for
 192 extracting a new set of features from the input array, b is the bias vector, and $h(\cdot)$ is the
 193 activation function. The shapes of X_l , W and T_l are (N, d) , (N, m) and $(N, d - m + 1)$,
 194 respectively. Several pooling layers are also applied between the convolutional layers
 195 for increasing the area covered by the next receptive fields. The output of the final
 196 convolutional layer is then flattened and used as input of several stacked fully connected
 197 layers, which can be described as:

$$T_l = f_l(X_l | \Theta_l) = h(WX_l + b), \quad \Theta_l = [W, b] \quad (3)$$

198 In the case of multiclass classification, the number of neurons of the output layer is
 199 the number of classes. Using softmax as the activation function for the output layer,
 200 each output neuron indicates the membership degree of the input samples for each class.
 201 During the training process, the parameters of the network are adjusted according to the
 202 back-propagated classification error and the parameters of the network are optimized to
 203 minimize an appropriate loss function (Goodfellow et al., 2016).

204 The proposed topology aims a compact 1D CNN architecture with a reduced number
 205 of parameters. The number of parameters of a CNN is directly related to the compu-
 206 tational effort to train such a network as well as to the need of a large amount of data
 207 for training. Therefore, the proposed architecture shown in Figure 2 is made of four
 208 convolutional layers, possibly interlaced with max pooling layers, followed by two fully
 209 connected layers and an output layer. The baseline model shown in Figure 2 has as
 210 input an array of 16,000 dimensions, which represents 1-second of audio sampled at 16
 211 kHz. However, this is not a constraint since we can adapt the model for different audio
 212 lengths and sampling rates in two ways: (i) change the model architecture to adapt it
 213 to the characteristics of the audio inputs; (ii) padding or segmenting the audio piece to
 214 adapt it to the input dimensions of the network.

215 Several other configurations can also be derived from subtle modifications of the
 216 base model (shown in Figure 2) to adapt it to shorter or longer audio inputs, as shown
 217 in Table 1. This implies modifying the number of convolutional layers as well as the
 218 number and the dimension of filters and the stride. However, for long contiguous audio
 219 recordings, instead of increasing the input dimension of the network, which also implies
 220 increasing the number of parameters, and consequently its complexity, it is preferable to
 221 split the audio waveform into shorter frames by changing the window width as explained
 222 in Section 2.1. In this way, we keep the network compact and it can process audio
 223 waveforms of any length. In spite of that, in Section 3.2 we evaluate different audio
 224 lengths as input, keeping a fixed sampling rate of 16 kHz.

225 The proposed 1D CNN has large receptive fields in the first convolutional layers
 226 since it is assumed that the first layer should have a more global view of the audio
 227 signal. Moreover, the environmental sound signal is non-stationary *i.e.* the frequency
 228 or spectral contents of the signal changes with respect to time. Therefore, shorter filters
 229 do not provide a general view on the spectral contents of the signal. The output of

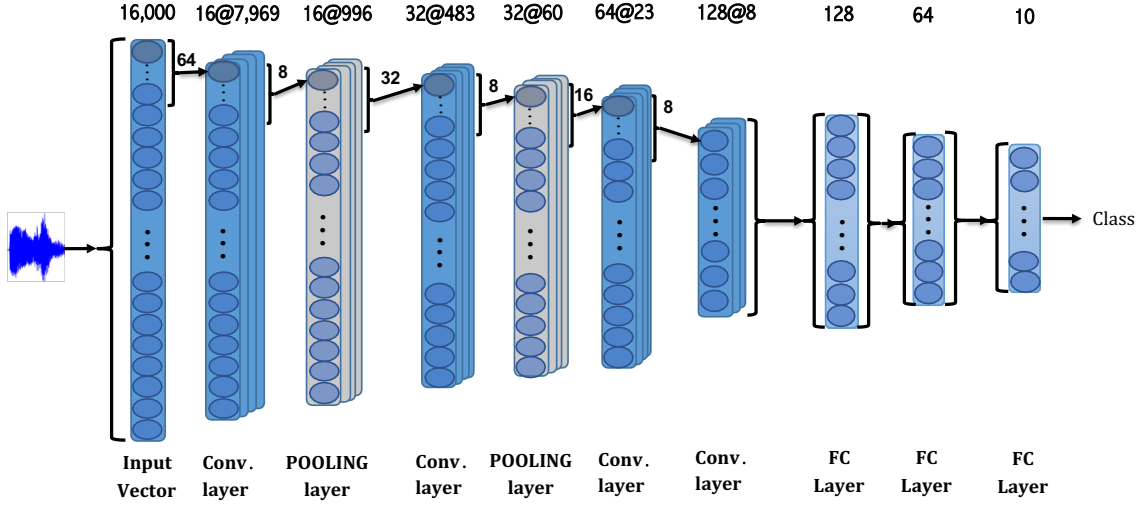


Figure 2: The architecture of the proposed end-to-end 1D CNN for environmental sound classification. The dimension, number of filters and filter size are given for the input size of 16,000. For other input sizes, the values are presented in Table 1.

Table 1: The configuration of the convolutional layers (CL) and pooling layers (PL) for the end-to-end CNN considering different input sizes (audio lengths).

Input Size		Layer							
		CL1	PL1	CL2	PL2	CL3	CL4	CL5	PL3
50,999	Dim	25,468	3,183	1,576	197	91	42	20	5
	# Filters	16	16	32	32	64	128	256	256
	Filter Size	64	8	32	8	16	8	4	4
	Stride	2	8	2	8	2	2	2	4
32,000	Dim	15,969	1,996	983	122	54	24	11	2
	# Filters	16	16	32	32	64	128	256	256
	Filter Size	64	8	32	8	16	8	4	4
	Stride	2	8	2	8	2	2	2	4
16,000	Dim	7,969	996	483	60	23	8	NA	NA
	# Filters	16	16	32	32	64	128	NA	NA
	Filter Size	64	8	32	8	16	8	NA	NA
	Stride	2	8	2	8	2	2	NA	NA
16,000G	Dim	15,489	19,36	953	119	52	23	NA	NA
	# Filters	64	64	32	32	64	128	NA	NA
	Filter Size	512	8	32	8	16	8	NA	NA
	Stride	1	8	2	8	2	2	NA	NA
8,000	Dim	3,969	496	233	29	7	NA	NA	NA
	# Filters	16	16	32	32	64	NA	NA	NA
	Filter Size	64	8	32	8	16	NA	NA	NA
	Stride	2	8	2	8	2	NA	NA	NA
1,600	Dim	785	392	189	94	44	NA	NA	NA
	# Filters	16	16	32	32	64	NA	NA	NA
	Filter Size	32	2	16	2	8	NA	NA	NA
	Stride	2	2	2	2	2	NA	NA	NA

NA: Not Applicable. G: First layer of the CNN initialized with Gammatone filterbank.

230 the last pooling layer for all feature maps is flattened and used as input to a fully
 231 connected layer. In order to reduce the over-fitting, batch normalization is applied after
 232 the activation function of each convolution layer (Ioffe & Szegedy, 2015). The last fully
 233 connected layer has ten neurons. Mean squared logarithmic error, defined in Equation
 234 4 is used as loss function (\mathcal{L}):

$$\mathcal{L} = \frac{1}{N} \sum_i^N \log\left(\frac{p_i + 1}{a_i + 1}\right)^2 \quad (4)$$

235 where p_i , a_i and N are the predicted class, the actual class, and the number of samples
 236 respectively.

237 For all input sizes shown in Table 1, after the last pooling layer, there are two fully
 238 connected layers with 128 and 64 neurons respectively on which a drop-out is applied
 239 with a probability of 0.25 for both layers (Srivastava et al., 2014). The ReLU activation
 240 function ($h(x) = \max(x, 0)$) is used for all layers, except for the output layer where a
 241 softmax activation function is used. Since the amount of data for training is limited, it is
 242 not feasible to use deeper architectures without significant over-fitting. By the use of the
 243 architecture shown in Figure 2, it is possible to omit a signal processing module because
 244 the network is powerful enough to extract relevant low-level and high-level information
 245 from the audio waveform.

246 The convolutional layers of the proposed architecture are inspired in Aytar et al.
 247 (2016) who proposed a CNN architecture (SoundNet) for learning sound representa-
 248 tions from unlabeled videos. The SoundNet (Aytar et al., 2016) learns multimodal
 249 features from audio and video using two concurrent CNNs which are further used with
 250 a SVM classifier. On the other hand, the proposed 1D CNN architecture learns the rep-
 251 resentation directly from the audio waveform, and it uses such a learned representation
 252 as input to a fully connected neural network for classification.

253 *2.3. Gammatone Filterbanks*

254 Another interesting characteristic of such a 1D CNN is that its first layer can be ini-
 255 tialized as a Gammatone filter bank. A Gammatone filter is a linear filter described by
 256 an impulse response of a gamma distribution and a sinusoidal tone. This initialization
 257 can be viewed as a trade-off between handcrafted features and representation learning.
 258 In this configuration, the kernels of the first layer are initialized by 64 band-pass Gam-
 259 matone filters with central frequency ranging from 100 Hz to 8 kHz. Such a filterbank
 260 decomposes the input signal into 64 frequency bands.

261 Gammatone filters have been used in models of the human auditory system and are
 262 physiologically motivated to simulate the structure of peripheral auditory processing
 263 stage. For this reason, Gammatone filters have also been used to initialize the first layer
 264 of 1D CNNs for automatic speech recognition (Hoshen et al., 2015; Zeghidour et al., 2018;
 265 Sainath et al., 2015). Figure 3 illustrates the frequency response of the Gammatone
 266 filterbank, generated by the Gammatone-like spectrograms toolbox developed by Ellis
 267 (2009).

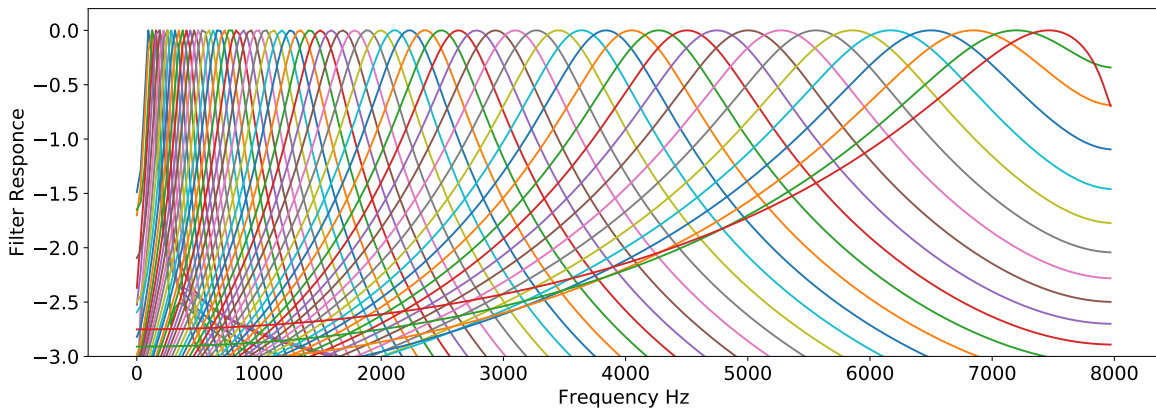


Figure 3: Frequency response of 64 filters of Gammatone filterbank.

268 *2.4. Aggregation of Audio Frames*

269 In the case where the input audio waveform X is split into S frames denoted as
 270 X_1, X_2, \dots, X_S , during the classification we need to aggregate the CNN predictions to
 271 come up to a decision on X , as illustrated in Figure 4. For such an aim, different fusion
 272 rules can be used to reach a final decision, such as the majority vote or the *sum* rule,
 273 which are denoted in Equations 5 and 6 respectively.

$$y_i = \sum_{j=1}^S o_{ji} \quad (5)$$

274 where o is the CNN prediction for the $j = 1, \dots, S$ segment of the audio waveform X
 275 and $i = 1, \dots, K$ is the predicted class. S is the number of frames and K is the number
 276 of classes.

$$y_i = \frac{1}{S} \sum_{j=1}^S o_{ji} \quad (6)$$

277 When there are K classes, we generate K values and them for an audio input, we
 278 choose the class with the maximum y_i value:

$$\text{Choose } C_i \text{ if } y_i = \max_{k=1}^K y_k \quad (7)$$

279 **3. Experimental Results**

280 The proposed end-to-end 1D CNN for environmental sound classification was eval-
 281 uated on the UrbanSound8k dataset (Salamon et al., 2014). This dataset consists of
 282 8,732 audio clips summing up to 7.3 hours of audio recordings. The maximum duration
 283 of audio clips is four seconds. The classes and the number of samples in each class are:
 284 "Air conditioner (AI): 1000", "Car horn (CA): 429", "Children playing (CH): 1000",

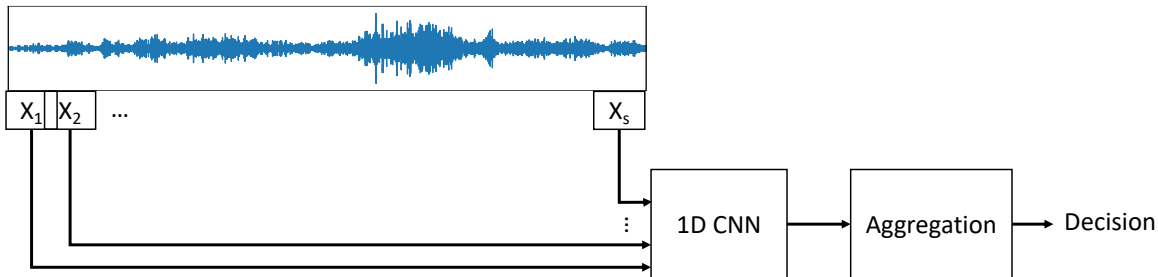


Figure 4: Aggregation of the predictions on the audio frames.

285 "Dog bark (DO): 1000", "Drilling (DR): 1000", "Engine (EN) idling: 1000", "Gun shot
 286 (GU): 374", "Jackhammer (JA): 1000", "Siren (SI): 929", "Street music (ST): 1000".
 287 The original audio clips are recorded at different sample rates. For the experiments
 288 presented in this paper, they have been downsampled to 16 kHz in order to unify the
 289 shape of the input signal for the 1D CNN.

290 3.1. Fine-Tuning the 1D CNN Architecture

291 The number of convolutional layers plays a key role in detecting high-level concepts.
 292 The number of convolutional layers for the base model shown in Figure 2 was deter-
 293 mined in an exploratory experiment using the audio files of the UrbanSound8k dataset.
 294 The audio files were segmented into 16,000 samples and successive frames have 50% of
 295 overlapping. Ten percent of the dataset was used as validation set and 10% percent of
 296 the dataset was also used as test set. Each network was trained with 80% of the dataset
 297 up to 100 epochs with batch sizes of 100 samples. The accuracy achieved by the 1D
 298 CNN with one to four convolutional layers on test set was 69%, 75%, 79% and 80%,
 299 respectively. Four convolutional layers is the upper limit since the minimal dimension of
 300 the feature map has been reached at this layer. The same procedure was also adopted
 301 to find the best number of convolution layers as well as their parameters for the other
 302 configurations derived from the base model which are described in Table 1.

303 3.2. Evaluation on Different Audio Lengths

304 All experiments reported in this subsection used a 10-fold cross-validation procedure
 305 to produce a fair comparison with the results reported by Salamon et al. (2014). One
 306 of the nine training folds is used as validation set for optimizing the parameters of the
 307 network to achieve the best accuracy. A batch size of 100 samples was used for training
 308 the CNNs and they were trained up to 100 epochs with early stopping. The Adadelta
 309 (Zeiler, 2012) optimizer with the default learning rate of 1.0 was used. Adadelta has
 310 been chosen because this method dynamically adapts the learning rate during the opti-
 311 mization process.

312 First, the proposed end-to-end 1D CNN is evaluated on different audio lengths to
 313 assess the impact of the input length on the classification performance. Next, the full
 314 audio recordings of UrbanSound8k dataset, which have 50,999 frames (\approx three seconds),

315 were also segmented into shorter frames using a sliding window and considering different
 316 overlapping percentages (0%, 25%, 50%, and 75%). The architecture shown in Figure 2
 317 was adapted according to the parameters described in Table 1, leading to audio frames
 318 of 1,600 (≈ 100 msec), 8,000 (≈ 500 msec), 16,000 (≈ 1 second) and 32,000 samples (\approx
 319 2 seconds).

320 The process of segmenting the audio signal into frames and aggregating the predic-
 321 tions of the classifier for all frames, resembles the process of aggregating the prediction
 322 of ensemble of classifiers. In this process, the most important parts of the audio sig-
 323 nal contribute more to the final decision while the noisy or outlier frames have their
 324 importance averaged during the aggregation process. Table 2 shows the best results
 325 achieved with different frame sizes, window overlapping and combination rules on the
 326 UrbanSound8k dataset in terms of mean accuracy. For the classification of each test
 327 sample of the original dataset, the predictions for each audio segment are combined us-
 328 ing either the majority voting or the sum rule (Kittler et al., 1998). Table 2 shows that
 329 the 16,000-input architecture achieved the highest accuracy which is the same accuracy
 330 achieved by 1D CNN with 50,999 inputs, even if it has almost twice less parameters
 331 than that network. Furthermore, the 8,000-input architecture achieved a mean accu-
 332 racy close to that, even if it has almost three times less parameters. If we increase the
 333 input size from one second to two or more seconds, besides increasing the number of
 334 parameters of the models, we reduce the number of audio segments, which may affect
 335 the training of such models due to the reduced amount of data. For this reason, we do
 336 not observe any improvement for audio segments beyond one second (16,000 frames).
 337 On the other hand, for the 1,600-input architecture, the mean accuracy is about 6%
 338 lower than the best architectures. This is an indication that short audio segments do
 339 not contain enough information to train properly the 1D CNN. However, this behaviour
 340 may be particular for the UrbanSound8k dataset and it cannot be generalized to other
 341 audio classification tasks or datasets. Table 2 also shows the computational time per
 342 epoch for training the networks with a subset 10,000 audio segments. The input size
 343 has also a direct relationship with training time, as more operations need to be done for
 344 larger inputs. Therefore, the 16,000-input CNN provides the best tradeoff between the
 345 number of parameters of network, computational time and mean accuracy.

Table 2: Mean accuracy and standard deviation on the UrbanSound8k dataset over the 10 folds for the different architectures (input dimensions) and 50% overlapping.

Input Dimension	Combination Rule	Mean\pmSD Accuracy	# of Parameters	Computational Time (Sec)
50,999	NA	83% \pm 1.3%	421,146	3.917
32,000	Maj Voting	82% \pm 0.9%	322,842	3.325
16,000	Sum Rule	83% \pm 1.3%	256,538	1.863
8,000	Sum Rule	80% \pm 1.9%	116,890	1.073
1,600	Sum Rule	77% \pm 3.0%	394,906	0.648

NA: Not applicable

346 The box-plot of Figure 5 also shows that the 16,000-input 1D CNN is the best choice

347 since it provides the highest median; the interquartile range is the smallest one; and
 348 there is no outlier. Furthermore, such an architecture has the same mean accuracy, but
 349 almost half of the number of parameters than the second-best choice, the 50,999-input
 350 1D CNN. Therefore, the 16,000-input 1D CNN is preferable over other architectures, as
 351 it presents the best trade-off between the number of parameters and accuracy.

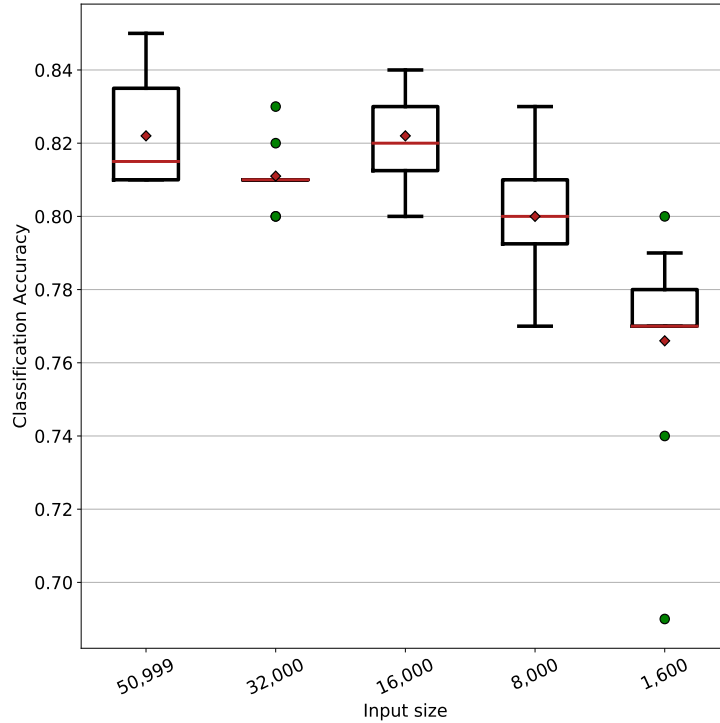


Figure 5: The box plot for the five different input sizes on UrbanSound8k dataset.

352 In order to have a better insight about the behavior of the convolutional filters
 353 learned by the proposed 1D CNN, the Fourier transform of some filters was computed
 354 and their frequency responses are shown in Figure 6. These filters were randomly ini-
 355 tialized and trained for the specific task and all of their parameters, such as central
 356 frequency, bandwidth, gain/attenuation, were learned directly from the data with the
 357 aim of minimizing a loss function. The learned filters are a combination of different
 358 (mainly band-pass and band-reject) filters with selective attenuation levels for different
 359 frequency levels. The filters of the first layers (CL1 and CL2) do not exhibit dominant
 360 frequencies and are quite noisy. On the other hand, the filters learned at the deeper
 361 layers (CL3 and CL4) are more regular filters, i.e., they have a well-defined frequency
 362 response which is closer to ideal filters. However, the resolution of the Fourier transform
 363 of the deeper layers is lower than in the initial layers because they are smaller than
 364 the initial ones. This analysis lead us to propose some enhancements to the proposed
 365 approach as an attempt to improve the response of the filters learned by the network.

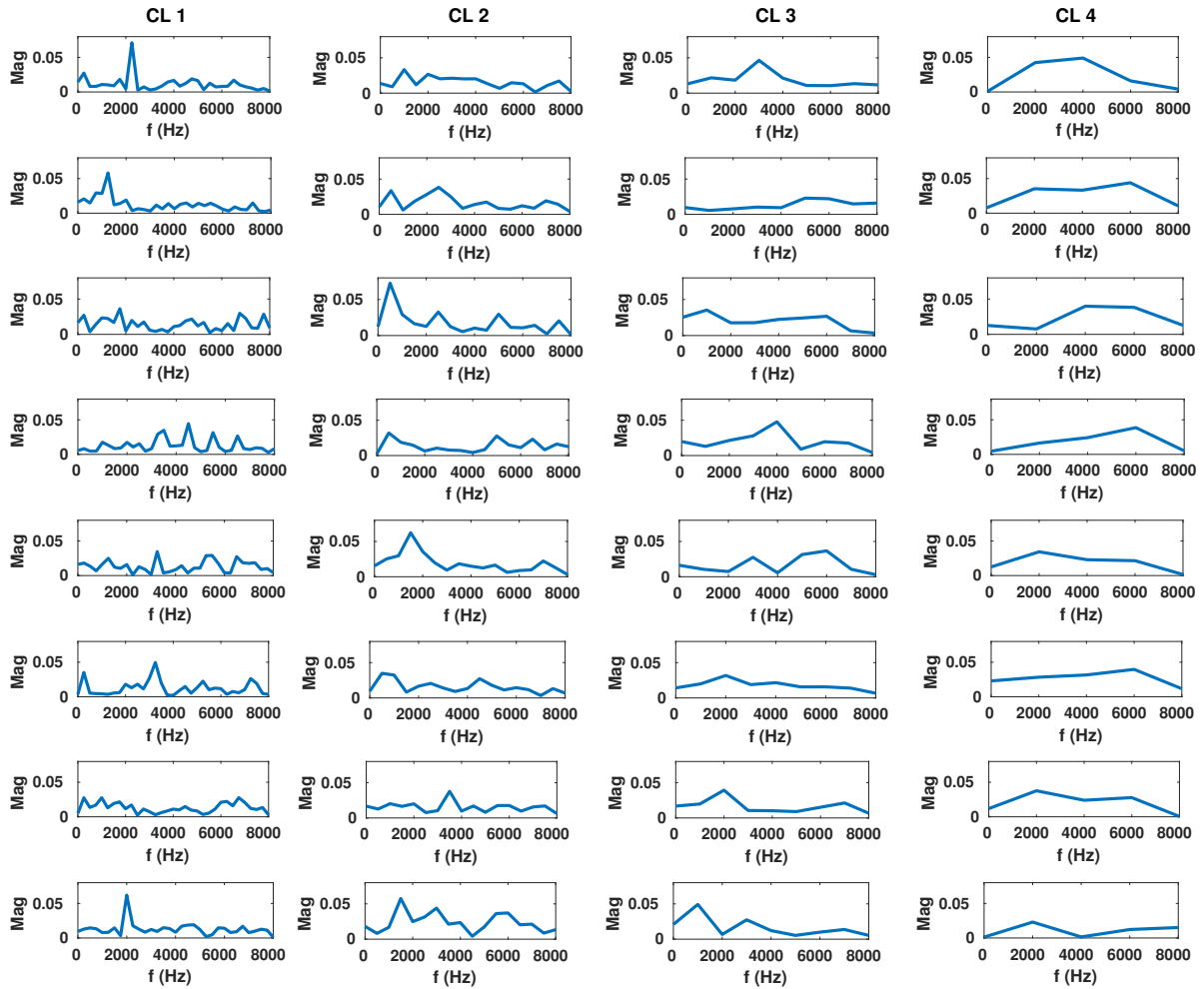


Figure 6: Fourier transform of randomly selected filters from the four convolutional layers (CLs) of the proposed 16,000-input 1D CNN shown in Figure 2.

366 *3.3. Architecture Enhancement*

367 Three enhancements to the proposed approach are evaluated: (i) replacing the Ham-
 368 ming sliding window by a rectangular window because the Hamming window smooths
 369 the signal and reduces the energy of the beginning and end of the audio frame and this
 370 may cause a loss of information; (ii) augmenting slightly the amount of training data by
 371 increasing the window overlapping during the audio segmentation; (iii) initializing the
 372 first convolutional layer as a Gammatone filterbank as described in Section 2, and make
 373 this layer non-trainable. During the training procedure, these filters can be modified by
 374 the forward and backward propagation. However, the best performance is achieved by
 375 making these filters non-trainable.

376 Table 3 summarizes the three proposed enhancements and their impact on the mean
 377 accuracy and on the computational time per epoch during training. The rectangular
 378 window leads to a slight improvement of 2% in the mean accuracy. Increasing the
 379 overlapping from 50% to 75% led to another 2% of improvement in the mean accuracy.
 380 Finally, initializing the first layer of such a 1D CNN with a Gammatone filterbank,
 381 also contributed to improve the mean accuracy in 2%, even if the number of parameters
 382 doubles due to the increase in the number of filters in such a layer. This also increases the
 383 training time. An important remark is that all these enhancements have also improved
 384 the performance of most of the other 1D CNN architectures presented in Table 1. In
 385 spite of that, the 16,000-input 1D CNN remains the one with the highest mean accuracy.

Table 3: Improvements in the mean accuracy for the 16,000-input 1D CNN on the UrbanSound8k dataset.

CL1 Initialization	Window	Overlapping	Combination Rule	Mean Accuracy	# of Parameters	Computation Time (Sec)
Randomly	Hamming	50%	Sum Rule	83%	256,538	1.863
Randomly	Rectangular	50%	Sum Rule	85%	256,538	1.863
Gammatone	Rectangular	50%	Sum Rule	87%	550,506	6.099
Randomly	Rectangular	75%	Sum Rule	87%	256,538	1.863
Gammatone	Rectangular	75%	Sum Rule	89%	550,506	6.099

386 Figure 7 shows the Fourier transform of some of the filters of the enhanced model
 387 with non-trainable Gammatone filterbank. Similar to the filters of the original model
 388 (Figure 6), the filters of the deepest layers (CL3 and CL4) have a well-defined frequency
 389 response. Filters of the intermediate layer (CL2) still do not exhibit dominant frequency
 390 levels. Even though, the minor changes in the responses of the intermediate and deeper
 391 filters, the Gammatone filters of the first layer were useful to improve the mean accuracy
 392 of the proposed 1D CNN.

393 **4. Discussion**

394 Table 4 shows the mean classification accuracy achieved by the proposed 1D CNN
 395 as well as the results achieved by other state-of-the-art approaches described in the
 396 literature. The proposed 1D CNN achieved a mean accuracy of 89% with a standard

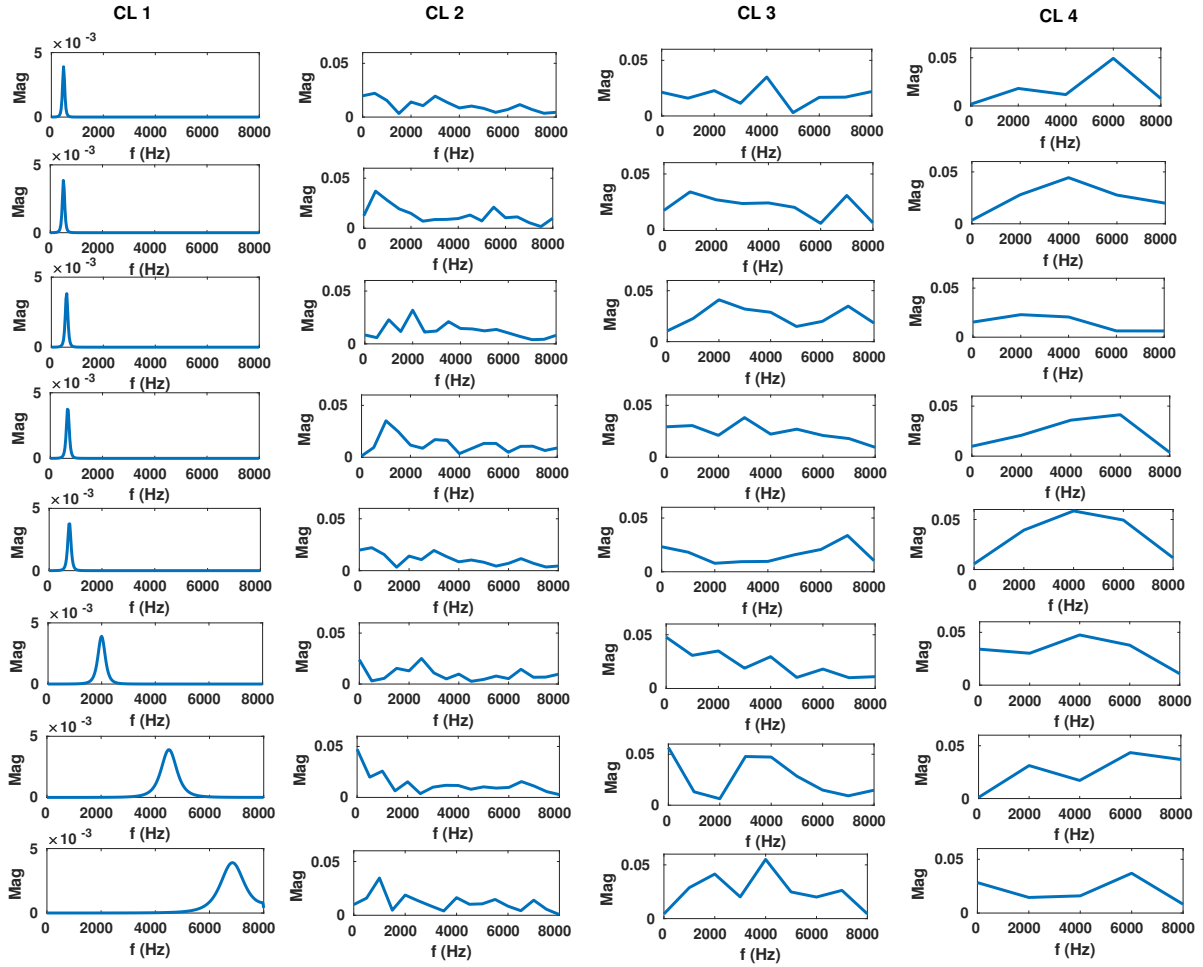


Figure 7: Fourier transform of randomly selected filters from the four convolutional layers (CLs) of the 16,000-input 1D CNN with Gammatone filterbank in the first convolutional layer of the network.

397 deviation of only 0.9% across the 10 folds. The proposed 1D CNN, the RawNet (Li et al.,
 398 2018), the EnvNet-v2 (Tokozume et al., 2017) and the M18 CNN (Dai et al., 2017) are
 399 end-to-end architectures, which learn the representation directly from the audio wave-
 400 form. DS-CNN is a combinational model, which uses both raw audio signal and 2D
 401 representations as input to a CNN. All other approaches in Table 4 use 2D representa-
 402 tions of the audio signal as input. As it is shown in Table 4, the proposed approach has
 403 lower number of parameters than most of the state-of-the-art approaches described in
 404 the literature and therefore it requires a relatively few number of samples for appropriate
 405 training. Furthermore, it is shown that the proposed algorithm outperforms all other
 406 approaches which use raw audio signal as input to the CNN. Therefore, the proposed
 407 approach is a quite suitable candidate to be used in ensemble models as described by Li
 408 et al. (2018). Figure 8 also compares the proposed 1D CNN with other approaches on
 409 UrbanSound8k dataset for environmental sound classification using a boxplot generated
 410 from the accuracy scores of 10 folds. Note that for some models the information about
 411 the accuracy scores of 10 folds was not available. So, only mean accuracy of the models
 412 are reported.

413 The proposed approach also does not require any signal processing module for feature
 414 extraction from audio signal. Therefore, it is suitable to be used in mobile or embedded
 415 devices. Moreover, as mentioned by Boddapati et al. (2017), the operation of generating
 416 2D representations from audio signal is time-consuming. For instance, producing spec-
 417 trograms of ESC-50 (Piczak, 2015b) dataset which consists of 2,000 samples takes five
 418 minutes. Generating corresponding MFCC features also takes five minutes. In addition
 419 to that, producing CRP representations takes 24 hours. Also, 2D representations can
 420 not be computed on GPU due to lack of suitable libraries. This issue makes models
 421 based on 2D representations impractical for real-time applications.

422 Moreover, approaches based on 2D representations are much more vulnerable to
 423 adversarial attacks which can easily fool these models. As it is shown by Esmailpour
 424 et al. (2019a), the models based on 2D representations can be easily fooled by adversarial
 425 attacks originally designed to fool image processing models. They have also pointed out
 426 that generalizing the current attacks to raw audio signals is not feasible because of the
 427 high-dimensionality of raw audio signals.

428 Figure 9 shows the confusion matrix of the proposed end-to-end 1D CNN on the
 429 UrbanSound8k dataset. Values along the diagonal indicate the number of samples clas-
 430 sified correctly for each specific class. It shows that the ST and CH classes are the
 431 hardest classes for the CNN. However, EN and GU classes are well separated by the
 432 proposed CNN.

433 *4.1. Filter Response*

434 The magnitude responses of the convolutional filters of the first layer of the pro-
 435 posed 1D CNN are shown in Figure 10. To obtain a better image representation of
 436 the frequency response, the number of kernels in the first layer has been increased to
 437 64 (compared to 16 in the one used in the experiments). Note that this configuration
 438 led to a slight decrease in the classification accuracy. Figures 10(a) and 10(b) show the

Table 4: Mean accuracy of different approaches on the UrbanSound8k dataset.

Approach	Representation	Mean Accuracy	# of Parameters
TSCNN-DS (Su et al., 2019)	2D	97%	15.9 M
GoogLeNet (Boddapati et al., 2017)	2D	93%	6.7 M
MelNet (Li et al., 2018)	2D	90%	211 k
SB-CNN (DA) (Salamon & Bello, 2017)	2D	79%	241 k
SKM (DA) (Salamon & Bello, 2015)	2D	76%	NA
SKM (Salamon & Bello, 2015)	2D	74%	NA
PiczakCNN (Piczak, 2015a)	2D	73%	26 M
SB-CNN (Salamon & Bello, 2017)	2D	73%	241 k
VGG (Pons & Serra, 2018)	2D	70%	77 M
DS-CNN (Li et al., 2018)	1D-2D	92%	NA
Proposed 1D CNN Gamma	1D	89%	550 k
RawNet (Li et al., 2018)	1D	87%	377 k
Proposed 1D CNN Rand	1D	87%	256 k
EnvNet-v2 (Tokozume et al., 2017)	1D	78%	101 M
M18 CNN (Dai et al., 2017)	1D	72%	3.7 M

NA: Not available. DA: With data augmentation.

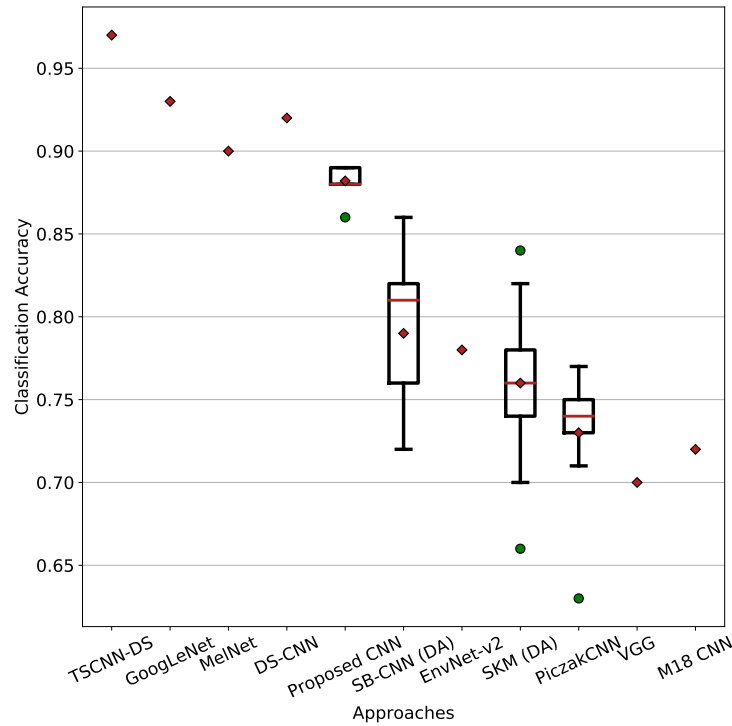


Figure 8: Classification accuracy of the proposed 1D CNN as well as the results obtained by other state-of-the-art approaches. Some parts of figure adapted from (Salamon & Bello, 2017).

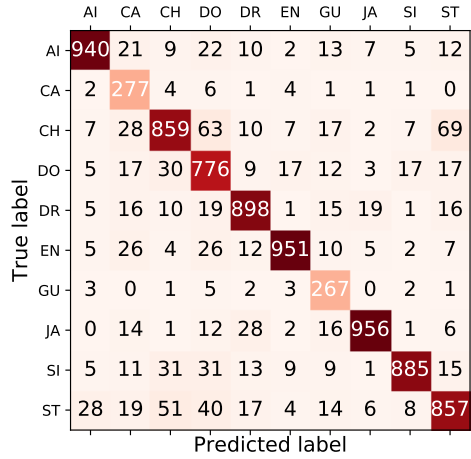


Figure 9: Confusion matrix for the proposed end-to-end 1D CNN.

439 response of the filters after convergence and the response of the kernels sorted based on
 440 their central frequencies, respectively. The central frequency of each kernel is computed
 441 by computing the Fast Fourier transform of the filter and by selecting the frequency bin
 442 with the highest peak. Each row in the image is created by feeding the network with a
 443 sinusoidal wave with a specific frequency. For such an aim, sinusoidal waves in the range
 444 of 1 Hz to 8 kHz, with a step of 100 Hz, have been used. The feature map of the first
 445 convolutional layer is first obtained and then, it is computed the average of the feature
 446 map along the time axis. Figure 10(c) shows the output of 64 Gammatone filters used
 447 as band-pass filters.

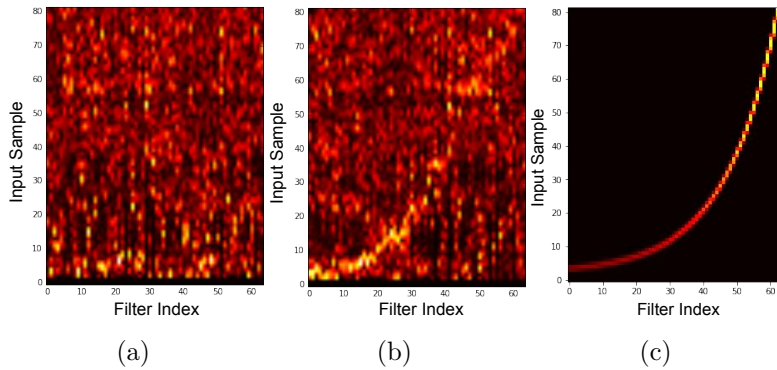


Figure 10: Magnitude response of the convolutional filters of the first layer of the end-to-end 1D CNN: (a) response of the filters after convergence; (b) response of the kernels after sorting based on their central frequency; (c) frequency response of band pass filters. Center frequency of filters are selected according to constant Q transform rules (Brown, 1991).

448 From Figure 10(b), it can be seen that the learned filters have a logarithmic response

449 similar to the band pass filters created using cardinal sinusoidal functions. In addition,
450 this behavior is also similar to how humans perceive sounds, which is also logarithmic
451 (Roederer, 2008). A similar behavior has also been observed in other end-to-end systems
452 for audio processing tasks (Hoshen et al., 2015; Sainath et al., 2015; Tokozume & Harada,
453 2017).

454 5. Conclusion

455 In this paper, an end-to-end 1D CNN for environmental sound classification has been
456 proposed. The architecture of the network consists of three to five convolutional layers,
457 depending on the length of the audio signal. The proposed end-to-end CNN learns the
458 representation directly from the audio signal. The proposed approach was evaluated on
459 a dataset of 8,732 audio samples and the experimental results have shown that the pro-
460 posed end-to-end approach learns several relevant filter representations which allows it
461 to outperform most of state-of-the-art approaches based on 2D representations and 2D
462 CNNs. It also performs better than all models that use raw audio signal as input and
463 use UrbanSound8k dataset (Salamon et al., 2014) for environmental sound classifica-
464 tion. Furthermore, the proposed end-to-end 1D architecture has fewer parameters than
465 most of the other CNN architectures for environmental sound classification. Moreover,
466 the proposed approach does not require any signal processing module for audio classi-
467 fication, which makes this model quite suitable to be used in mobile sound recognition
468 applications or in embedded systems.

469 However, even if we have achieved the best results using 1D representation of the
470 audio signal, it may have a complementarity between the learned 1D filters and the filters
471 learned from 2D representations (spectrograms), at least for some classes. This is an
472 indication that the overall performance may be improved by combining the approaches
473 that use 1D and 2D representations similar to the ensemble model proposed by Li et al.
474 (2018). As a future work, we will investigate if such a combination is feasible and if
475 it can lead to a better performance in classifying environmental sounds. Furthermore,
476 the filters learned in the intermediate convolutional layers of the proposed 1D CNN
477 do not exhibit dominant frequencies and seems to be noisy. A further investigation is
478 necessary to find out how to circumvent such a problem and possibly improve further
479 the performance of the proposed 1D CNN.

480 Availability of Data and Material

481 UrbanSound8k dataset (Salamon et al., 2014) is used for training and testing the
482 method. The dataset is available online ². and the source code of the proposed end-to-
483 end CNN will also be made available in the final version of the paper.

²<https://urbansounddataset.weebly.com/urbansound8k.html>

484 **Competing Interests**

485 The authors declare that they have no competing interests.

486 **Credit Authorship Contribution Statement**

487 **Sajjad Abdoli:** Conceptualization, Methodology, Software, Validation, Formal
488 Analysis, Investigation, Data Curation, Writing – Original Draft, Visualization. **Patrick**
489 **Cardinal and Alessandro Lameiras Koerich:** Conceptualization, Methodology,
490 Validation, Formal Analysis, Investigation, Resources, Data Curation, Writing – Re-
491 view & Editing, Supervision, Project Administration, Funding Acquisition.

492 **Acknowledgements**

493 This work was funded by the Natural Sciences and Engineering Research Council of
494 Canada (NSERC). This work was also supported by the NVIDIA GPU Grant Program.

495 **References**

- 496 Aytar, Y., Vondrick, C., & Torralba, A. (2016). Soundnet: Learning sound represen-
497 tations from unlabeled video. In *Advances in neural information processing systems*
498 (pp. 892–900).
- 499 Benetos, E., Lafay, G., Lagrange, M., & Plumbley, M. (2016). Detection of overlapping
500 acoustic events using a temporally-constrained probabilistic model. In *IEEE Interna-*
501 *tional Conference on Acoustics, Speech and Signal Processing* (pp. 6450–6454).
- 502 Bisot, V., Serizel, R., Essid, S., & Richard, G. (2016). Acoustic scene classification
503 with matrix factorization for unsupervised feature learning. In *IEEE International*
504 *Conference on Acoustics, Speech and Signal Processing* (pp. 6445–6449).
- 505 Boddapati, V., Petef, A., Rasmusson, J., & Lundberg, L. (2017). Classifying environ-
506 mental sounds using image recognition networks. *Procedia computer science*, *112*,
507 2048–2056.
- 508 Brown, J. C. (1991). Calculation of a constant Q spectral transform. *The Journal of*
509 *the Acoustical Society of America*, *89*, 425–434.
- 510 Chu, S., Narayanan, S., & Kuo, C. (2009). Environmental sound recognition with
511 time–frequency audio features. *IEEE Transactions on Audio, Speech, and Language*
512 *Processing*, *17*, 1142–1158.
- 513 Costa, Y., Oliveira, L., Koerich, A., Gouyon, F., & Martins, J. (2012). Music genre
514 classification using LBP textural features. *Signal Processing*, *92*, 2723–2737.

- 515 Costa, Y. M., Oliveira, L. S., & Silla, C. N. (2017). An evaluation of Convolutional
516 Neural Networks for music classification using spectrograms. *Applied Soft Computing*,
517 *52*, 28–38. doi:10.1016/j.asoc.2016.12.024.
- 518 Costa, Y. M. G., Oliveira, L. E. S., Koerich, A. L., & Gouyon, F. (2011). Music genre
519 recognition using spectrograms. In *18th International Conference on Systems, Signals*
520 *and Image Processing* (pp. 1–4).
- 521 Dai, W., Dai, C., Qu, S., Li, J., & Das, S. (2017). Very Deep Convolutional Neural
522 Networks for Raw Waveforms. In *IEEE International Conference on Acoustics, Speech*
523 *and Signal Processing (ICASSP)* (pp. 421–425).
- 524 Dieleman, S., & Schrauwen, B. (2014). End-to-end learning for music audio. In *IEEE*
525 *International Conference on Acoustics, Speech and Signal Processing (ICASSP)* (pp.
526 6964–6968).
- 527 Ellis, D. P. W. (2009). *Gammatone-like spectrograms, web resource..* URL: [http:
528 //www.ee.columbia.edu/~dpwe/resources/matlab/gammatonegram/](http://www.ee.columbia.edu/~dpwe/resources/matlab/gammatonegram/).
- 529 Esmaeilpour, M., Cardinal, P., & Koerich, A. L. (2019a). A robust approach for securing
530 audio classification against adversarial attacks. *arXiv preprint arXiv:1904.10990*, (pp.
531 1–14).
- 532 Esmaeilpour, M., Cardinal, P., & Koerich, A. L. (2019b). Unsupervised feature learning
533 for environmental sound classification using cycle consistent generative adversarial
534 network. *arXiv preprint arXiv:1904.04221*, (pp. 1–34).
- 535 Garofolo, J. S., Lamel, L. F., Fisher, W. M., Fiscus, J. G., & Pallett, D. S. (1993).
536 Darpa timit acoustic-phonetic continous speech corpus cd-rom. nist speech disc 1-1.1.
537 *NASA STI/Recon technical report n, 93*.
- 538 Geiger, J., & Helwani, K. (2015). Improving event detection for audio surveillance
539 using Gabor filterbank features. In *23rd European Signal Processing Conference* (pp.
540 714–718).
- 541 Goodfellow, I., Bengio, Y., Courville, A., & Bengio, Y. (2016). Deep learning. MIT
542 Press Cambridge volume 1.
- 543 He, K., Zhang, X., Ren, S., & Sun, J. (2016). Deep residual learning for image recogni-
544 tion. In *Proceedings of the IEEE conference on computer vision and pattern recognition*
545 (pp. 770–778).
- 546 Hershey, S., Chaudhuri, S., Ellis, D., Gemmeke, J., Jansen, A., Moore, R., Plakal, M.,
547 Platt, D., Saurous, R., Seybold, B. et al. (2017). Cnn architectures for large-scale
548 audio classification. In *International Conference on Acoustics, Speech and Signal*
549 *Processing (ICASSP)* (pp. 131–135).

- 550 Hoshen, Y., Weiss, R. J., & Wilson, K. W. (2015). Speech acoustic modeling from raw
551 multichannel waveforms. In *IEEE International Conference on Acoustics, Speech and*
552 *Signal Processing (ICASSP)* (pp. 4624–4628).
- 553 Hu, J., Shen, L., & Sun, G. (2018). Squeeze-and-excitation networks. In *Proceedings of*
554 *the IEEE conference on computer vision and pattern recognition* (pp. 7132–7141).
- 555 Ioffe, S., & Szegedy, C. (2015). Batch normalization: Accelerating deep network training
556 by reducing internal covariate shift. In *International Conference on Machine Learning*
557 (pp. 448–456).
- 558 Kim, T., Lee, J., & Nam, J. (2018). Sample-level cnn architectures for music auto-
559 tagging using raw waveforms. In *IEEE International Conference on Acoustics, Speech*
560 *and Signal Processing (ICASSP)* (pp. 366–370).
- 561 Kittler, J., Hatef, M., Duin, R. P., & Matas, J. (1998). On combining classifiers. *IEEE*
562 *transactions on pattern analysis and machine intelligence*, *20*, 226–239.
- 563 Laffitte, P., Wang, Y., Sodoyer, D., & Girin, L. (2019). Assessing the performances
564 of different neural network architectures for the detection of screams and shouts in
565 public transportation. *Expert Systems with Applications*, *117*, 29–41.
- 566 Li, S., Yao, Y., Hu, J., Liu, G., Yao, X., & Hu, J. (2018). An ensemble stacked con-
567 volutional neural network model for environmental event sound recognition. *Applied*
568 *Sciences*, *8*, 1152.
- 569 Ludeña-Choez, J., & Gallardo-Antolín, A. (2016). Acoustic event classification using
570 spectral band selection and non-negative matrix factorization-based features. *Expert*
571 *Systems with Applications*, *46*, 77–86.
- 572 McFee, B., Humphrey, E., & Bello, J. (2015). A software framework for musical data
573 augmentation. In *International Society for Music Information Retrieval Conference*
574 (pp. 248–254).
- 575 Mesaros, A., Heittola, T., Dikmen, O., & Virtanen, T. (2015). Sound event detection in
576 real life recordings using coupled matrix factorization of spectral representations and
577 class activity annotations. In *IEEE International Conference on Acoustics, Speech*
578 *and Signal Processing (ICASSP)* (pp. 151–155).
- 579 Mulimani, M., & Koolagudi, S. G. (2019). Segmentation and characterization of acoustic
580 event spectrograms using singular value decomposition. *Expert Systems with Appli-*
581 *cations*, *120*, 413–425.
- 582 Mydlarz, C., Salamon, J., & Bello, J. (2017). The implementation of low-cost urban
583 acoustic monitoring devices. *Applied Acoustics*, *117*, 207–218.

- 584 Piczak, K. (2015a). Environmental sound classification with convolutional neural net-
585 works. In *25th International Workshop on Machine Learning for Signal Processing*
586 (pp. 1–6).
- 587 Piczak, K. J. (2015b). Esc: Dataset for environmental sound classification. In *Pro-*
588 *ceedings of the 23rd ACM international conference on Multimedia* (pp. 1015–1018).
589 ACM.
- 590 Pons, J., & Serra, X. (2018). Randomly weighted cnns for (music) audio classification.
591 *arXiv preprint*, . URL: <https://arxiv.org/pdf/1805.00237.pdf>.
- 592 Radhakrishnan, R., Divakaran, A., & Smaragdis, A. (2005). Audio analysis for surveil-
593 lance applications. In *IEEE Workshop on Applications of Signal Processing to Audio*
594 *and Acoustics* (pp. 158–161).
- 595 Ravanelli, M., & Bengio, Y. (2018). Speaker recognition from raw waveform with sincnet.
596 In *2018 IEEE Spoken Language Technology Workshop (SLT)* (pp. 1021–1028). IEEE.
- 597 Roederer, J. G. (2008). The physics and psychophysics of music: an introduction.
598 Springer Science & Business Media.
- 599 Sainath, T. N., Weiss, R. J., Senior, A., Wilson, K. W., & Vinyals, O. (2015). Learning
600 the speech front-end with raw waveform cldnns. In *Sixteenth Annual Conference of*
601 *the International Speech Communication Association* (pp. 1–5).
- 602 Salamon, J., & Bello, J. (2015). Unsupervised feature learning for urban sound classifi-
603 cation. In *IEEE International Conference on Acoustics, Speech and Signal Processing*
604 (pp. 171–175).
- 605 Salamon, J., & Bello, J. (2017). Deep convolutional neural networks and data augmen-
606 tation for environmental sound classification. *IEEE Signal Processing Letters*, *24*,
607 279–283.
- 608 Salamon, J., Jacoby, C., & Bello, J. (2014). A dataset and taxonomy for urban sound
609 research. In *22nd ACM International Conference on Multimedia* (pp. 1041–1044).
610 New York, NY, USA.
- 611 Sigtia, S., Stark, A., Krstulović, S., & Plumbley, M. (2016). Automatic environmental
612 sound recognition: Performance versus computational cost. *IEEE/ACM Transactions*
613 *on Audio, Speech, and Language Processing*, *24*, 2096–2107.
- 614 Simonyan, K., & Zisserman, A. (2014). Very deep convolutional networks for large-scale
615 image recognition. *arXiv preprint*, . URL: <https://arxiv.org/pdf/1409.1556.pdf>.
- 616 Srivastava, N., Hinton, G., Krizhevsky, A., Sutskever, I., & Salakhutdinov, R. (2014).
617 Dropout: a simple way to prevent neural networks from overfitting. *Journal of Ma-*
618 *chine Learning Research*, *15*, 1929–1958.

- 619 Stowell, D., Giannoulis, D., Benetos, E., Lagrange, M., & Plumbley, M. (2015). Detec-
620 tion and classification of acoustic scenes and events. *IEEE Transactions on Multime-*
621 *dia*, *17*, 1733–1746.
- 622 Stowell, D., & Plumbley, M. D. (2014). Automatic large-scale classification of bird
623 sounds is strongly improved by unsupervised feature learning. *PeerJ*, *2*, e488.
624 doi:<https://doi.org/10.7717/peerj.488>.
- 625 Su, Y., Zhang, K., Wang, J., & Madani, K. (2019). Environment sound classification
626 using a two-stream cnn based on decision-level fusion. *Sensors*, *19*, 1733.
- 627 Tokozume, Y., & Harada, T. (2017). Learning environmental sounds with end-to-end
628 convolutional neural network. In *IEEE International Conference on Acoustics, Speech*
629 *and Signal Processing (ICASSP)* (pp. 2721–2725).
- 630 Tokozume, Y., Ushiku, Y., & Harada, T. (2017). Learning from between-class examples
631 for deep sound recognition. *arXiv preprint*, . URL: [https://arxiv.org/pdf/1711.](https://arxiv.org/pdf/1711.10282.pdf)
632 [10282.pdf](https://arxiv.org/pdf/1711.10282.pdf).
- 633 Xie, J., & Zhu, M. (2019). Investigation of acoustic and visual features for acoustic
634 scene classification. *Expert Systems with Applications*, *126*, 20–29.
- 635 Zeghidour, N., Usunier, N., Synnaeve, G., Collobert, R., & Dupoux, E. (2018). End-
636 to-end speech recognition from the raw waveform. *arXiv preprint*, . URL: [https:](https://arxiv.org/pdf/1806.07098.pdf)
637 [//arxiv.org/pdf/1806.07098.pdf](https://arxiv.org/pdf/1806.07098.pdf).
- 638 Zeiler, M. (2012). Adadelta: an adaptive learning rate method. *arXiv preprint*, . URL:
639 <https://arxiv.org/pdf/1212.5701.pdf>.
- 640 Zhu, Z., Enge, J. H., & Hannun, A. (2016). Learning multiscale features directly from
641 waveforms. *Proceedings of the Annual Conference of the International Speech Com-*
642 *munication Association (INTERSPEECH)*, (pp. 1305–1309).